Muon-Catalyzed pt Fusion

P. Baumann, H. Daniel, S. Grunewald, F. J. Hartmann, R. Lipowsky, E. Moser, W. Schott, and T. von Egidy
Physik-Department, Technische Universität München, D-8046 Garching, Germany

P. Ackerbauer, W. H. Breunlich, M. Fuchs, M. Jeitler, P. Kammel, J. Marton, N. Nägele, J. Werner, and J. Zmeskal
Österreichische Akademie der Wissenschaften, Institut für Mittelenergiephysik, A-1090 Vienna, Austria

H. Bossy and K. M. Crowe
Lawrence Berkeley Laboratory, Berkeley, California 94720

R. H. Sherman
Los Alamos National Laboratory, Los Alamos, New Mexico 87545

K. Lou and C. Petitjean
Paul Scherrer Institut, CH-5232 Villigen, Switzerland

V. E. Markushin
Kurchatov Atomic Energy Institute, Moscow 123182, Russia
(19 February 1993)

Gamma rays and, for the first time, conversion muons of pt fusion have been measured from liquid mixtures of protium, deuterium, and tritium. The rate λ_{10} for spin flip from the triplet to the singlet state of $t\mu(1s)$ was found to be $\lambda_{10} = (1.06 \pm 0.13) \times 10^3 \mu\text{s}^{-1}$, the rate for muon-catalyzed pt fusion from the $(I = 1)$ nuclear-spin state to be $\lambda^f_{pt}(I = 1) = 0.067 \pm 0.002 {}^{+0.005}_{-0.002}\ \mu\text{s}^{-1}$, and the molecular formation rate to be $\lambda^m_{pt} = (7.5 \pm\ 0.3\ {}^{+1.0}_{-0.3})\ \mu\text{s}^{-1}$ (all rates normalized to liquid hydrogen density).

PACS numbers: 36.10.Dr

Among the various fusion reactions induced by negative muons in a mixture of hydrogen isotopes muon-catalyzed pt fusion is a rather exotic one. Nevertheless its study brings a wealth of information on all kinds of processes in muonic atoms and molecules. The two main reaction channels in this fusion are

$$pt\mu \to (\mu^4\text{He}) + \gamma, \quad Q_{1s} = 19.825 \text{ MeV}\,, \tag{1}$$

$$pt\mu \to \mu_{\text{conv}} +^4 \text{He}, \quad Q = 19.814 \text{ MeV}\,. \tag{2}$$

Here Q_{1s} denotes the Q value with the μ^4He system in the ground state. The branching ratio B between reactions (2) and (1) strongly depends on the population of the hyperfine states of the $pt\mu$ molecule [1] and hence on the whole chain of reactions from Coulomb capture to molecular formation. In a protium-tritium mixture with small tritium concentration c_t, $t\mu$ atoms are mostly generated by transfer from the proton to the triton and therefore have an initial kinetic energy of about 45 eV. At the instant of formation the two hyperfine structure (HFS) states of $t\mu(1s)$ may be assumed to be statistically populated. In collisions with protons $pt\mu$ molecules are formed in different HFS states, the probability of generating the nuclear spin configurations $I = 0$ being dependent on the total spin F of the $t\mu$ atom [2]. Fusion by single γ emission is impossible for the $I = 0$ state, whereas it is expected to prevail for $I = 1$. Hence B is strongly influenced by the spin-flip reaction

$$t\mu(F = 1) + t \underset{c_t\lambda_{01}}{\overset{c_t\lambda_{10}}{\rightleftharpoons}} t\mu(F = 0) + t'. \tag{3}$$

Here λ_{10} and λ_{01} denote the spin-flip rates $t\mu(1s, F = 1) \to t\mu(1s, F = 0)$ and vice versa, respectively (all normalized to liquid hydrogen density). Since the HFS splitting $E(F = 1) - E(F = 0) = 0.237$ eV is large in comparison with the energy of thermal motion, the spin flip $F = 1 \to F = 0$ becomes irreversible for the thermalized $t\mu$ atoms. As a result, the fusion yields depend on the tritium concentration, the size of the effect being determined by the spin-flip rate λ_{10}. A corresponding effect for muon-catalyzed pd fusion, the "Wolfenstein-Gershtein effect," was predicted in 1961 [3] and verified by experiment shortly after [4]. The spin-flip rate has been calculated to be very large, $\lambda_{10} = 10^3\ \mu\text{s}^{-1}$ [5–7], which makes it possible to observe the effect at rather small tritium concentrations.

The rate λ_{10} and the speed of $t\mu$ thermalization are very important for the dt-fusion cycle, because for thermal $t\mu(1s)$ *resonant* $dt\mu$-molecule formation, which is very fast, takes place only from the singlet state [8]. The faster the thermalized $t\mu(1s)$ system reaches the singlet state the shorter the dt-fusion cycle and the more dt fusions may be catalyzed by one muon.

0031-9007/93/70(24)/3720(4)$06.00

The pt-fusion rates give information on the pt nuclear interaction corresponding to energies so low that they are inaccessible to other experiments such as those with protons impinging on tritium. The triplet fusion rate $\lambda_{pt}^{f}(I=1)$ is connected with the pt-reaction constant K_0 by the relation

$$\lambda_{pt}^{f}(I=1)=\tfrac{4}{3}K_0\rho_0, \tag{4}$$

where ρ_0 is the probability for p and t to be at zero distance in the ground state of $pt\mu$ [9].

The experiment was performed at the μE4 channel of Paul Scherrer Institute (PSI), Villigen, Switzerland. The relevant parts of the setup are shown in Fig. 1. Details may be found in Ref. [10]. The cubic target cell was machined from pure iron and coated with silver. The target was surrounded by a vacuum chamber for thermal insulation. Below the target a scintillation counter (μC) with an NE102A scintillator (diameter 50 mm, thickness 28 mm) was employed to stop and detect the conversion muons [reaction (2)]. The signals from this detector could be routed to enable detection of the muon-decay electron following the muon stop. Before the run an energy calibration had been performed with muons from the beam line, which for this purpose was set to the appropriate momentum. A bismuth germanium oxide (BGO) detector (diameter 3 in., thickness 3 in.) was positioned below μC. It mainly served to detect the high-energy γ rays from fusion. A scintillation counter telescope with counters El2, El3, and El3A signalled a muon stop. These counters were also able to detect decay electrons. There were additional scintillation counters for electrons and other charged particles (El4, El4R, and El4U), x-ray and γ detectors, and neutron counters.

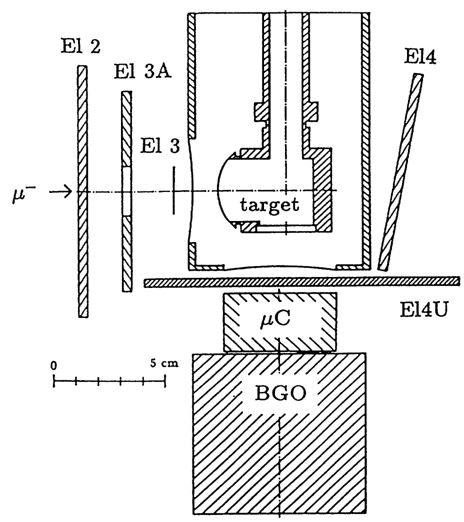

FIG. 1. Vertical cut of the setup. μC: conversion muon counter (NE 102A). BGO: γ ray detector (scintillation material $Bi_4Ge_3O_{12}$). El2, El3, El3A, El4, and El4U: counters for the detection of beam muons, electrons, and other charged particles (NE 102A). The electron counter EL4R, a Ge(hp) detector for high-energy gammas, a Ge(hp) x-ray detector, and two neutron counters are not shown. See text for further explanations.

The composition of the mixtures was analyzed with a quadrupole mass spectrometer [11]. Three different liquid-hydrogen fillings with small admixtures of deuterium and tritium were used in three different runs (EP1 to EP3, cf. Table I) to investigate the concentration dependent effects of reaction (3).

Events within 10 μs after muon stop were recorded on tape with as few hardware restrictions as possible so that time windows and thresholds could be set during data analysis. Background in the energy and time spectra generated from the incremental data was drastically reduced by excluding events in prompt coincidence with the muon stop (coincidence width 20 ns) and by requiring a decay electron to be registered by the electron counters as a sign that the muon had really stopped in the target filling [12].

The time distribution of the pt-fusion γ events can, at least for the runs EP1 and EP2, be well described by a biexponential function

$$f_{\mathrm{biexp}}(t)=A_b\exp(-\lambda_b t)+A_d\exp(-\lambda_d t) \tag{5}$$

with fitted parameters A_b, A_d, λ_b, and λ_d, see Table I.

Figure 2 presents a conversion-muon spectrum. Please note that the conversion-muon peak is shifted from 19 to 15 MeV because the conversion muons lose energy in the hydrogen filling and in the target windows. To clean the spectrum the stop of the muon in μC had to be in coincidence with a signal in El4U in front of μC. In addition, the decay electron had to produce a second signal in μC

TABLE I. Tritium concentration c_t, deuterium concentration c_d, data-taking time t_m, total stop events N_μ, buildup rates λ_b, and disappearance rates λ_d both for fusion γ rays and conversion muons, respectively. EP1, EP2, and EP3 denote different runs. χ^2_ν is the normalized χ^2 for the fits. The protium concentration c_p is given by $c_p = 1 - c_d - c_t$.

Run	EP1	EP2	EP3
c_t/%	0.81 ± 0.06	0.116 ± 0.006	0.0450 ± 0.0075
c_d/%	0.076 ± 0.005	0.0402 ± 0.0012	0.0365 ± 0.0055
t_m/h	19.5	48.3	54.7
N_μ	3.04×10^8	7.75×10^8	7.84×10^8
	BGO, γ rays from pt fusion		
λ_b/μs	6.49 ± 0.40	7.19 ± 0.22	5.22 ± 0.18
λ_d/μs	0.506 ± 0.005	0.520 ± 0.003	0.536 ± 0.005
χ^2_ν	0.965	1.04	1.27
	Muon counter, conversion muons		
λ_b/μs	6.70 ± 2.10	6.53 ± 0.95	5.13 ± 0.49
λ_d/μs	0.59 ± 0.05	0.62 ± 0.04	0.60 ± 0.03
χ^2_ν	1.01	1.30	1.16

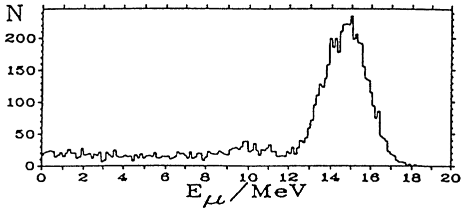

FIG. 2. Conversion-muon energy spectrum taken in run EP1. The coincidence conditions are described in the text. One channel corresponds to 127 keV.

and in the BGO between 0.2 μs and 3.0 μs after the first one. It had to deposit more than 1 MeV in μC. As soon as a pulse from El4U was in coincidence with this second signal the event was discarded. Time spectra taken with the muon counter can be described reasonably well by the biexponential function (5) (cf. Table I).

The spin-flip rate λ_{10} could be determined by taking into account only the processes following $t\mu$ formation. The experimentally determined branching ratios B were normalized to run EP1, the resulting $B_{\rm norm}$ values were compared with results from the computer code KIN [13,14]. This code uses Green's functions to solve the differential-equation system describing the problem with the reaction rates assumed to be constant in time. The molecular formation rates λ_{dt}^m=350 μs^{-1} [15], λ_{tt}^m=1.8 μs^{-1} [16], and λ_{pt}^m=7.5 μs^{-1} (see below) were used. The pt-fusion rates were assumed to be $\lambda_{pt}^f(I=1) = 0.067$ μs^{-1} (see below) and $\lambda_{pt}^f(I=0) = 0.0005$ μs^{-1} [17]. The branching ratios for the formation of the $pt\mu$ hyperfine states from the $t\mu(1s)$ hyperfine states were taken from [2]. Even large variations in all rates except λ_{10} changed the calculated $B_{\rm norm}$ values only slightly. Results from experiment and calculation are compared in Fig. 3. $B_{\rm norm}$ decreases with increasing tritium concentration. This is mainly caused by the growing influence of λ_{10}. To investigate thermalization effects $B_{\rm norm}$ was analyzed for different time windows. The idea is the following: Events shortly after muon stop (time window $0.02 \leq t/\mu s \leq 1.02$) are most probably coming from nonthermalized muonic tritium as the thermalization rate has a deep Ramsauer-Townsend minimum at 3 eV [18]. During that time the population of the $F=1$ state of $t\mu(1s)$ is held high by $F=0 \to F=1$ transitions as compared to late events ($4.02 \leq t/\mu s \leq 6.02$) where the $t\mu$ system may be assumed to be thermalized and $F=0 \to F=1$ transitions are no longer possible. Obviously the $B_{\rm norm}$ values change with delay time, much stronger than would be expected from calculations with constant rates. This clearly shows that an analysis with energy-dependent rates is needed. The value for λ_{10} found from the time window ($4.02 \leq t/\mu s \leq 6.02$) was $\lambda_{10} = (1.06 \pm 0.13) \times 10^3 \mu s^{-1}$. This value lies between older calculated values ($\lambda_{10} = 888$ μs^{-1} [5], $\lambda_{10} =$ 910 μs^{-1} [6]) and the most recent one ($\lambda_{10} = 1300$ μs^{-1} [7]).

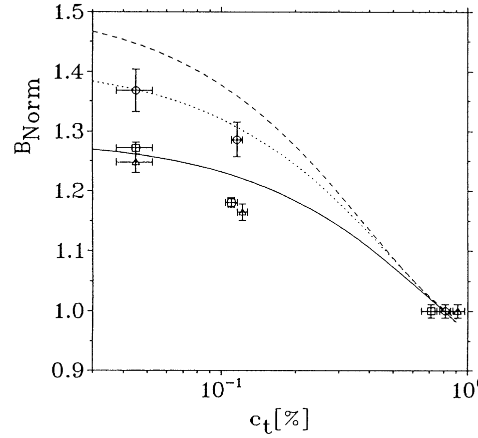

FIG. 3. Measured and calculated branching ratio $B_{\rm norm}$. Measured $B_{\rm norm}$: squares, circles, and triangles stand for time windows ($0.02 \leq t/\mu s \leq 8.02$), ($4.02 \leq t/\mu s \leq 6.02$), and ($0.02 \leq t/\mu s \leq 1.02$), respectively. Calculated $B_{\rm norm}$: dashed, dotted, and solid lines denote calculations with $\lambda_{10} = 500\,\mu s^{-1}$, $\lambda_{10} = 900\,\mu s^{-1}$, and $\lambda_{10} = 1300\,\mu s^{-1}$, respectively. The values for c_t=0.81% are separated horizontally to retain visibility.

To derive λ_{pt}^m and $\lambda_{pt}^f(I=1)$ all reactions including hyperfine transitions have been taken into account and pt-fusion γ time spectra were compared with results from the code KIN. Up to three time spectra (each with 300 channels at a 16 ns binning) have been fitted simultaneously with five free parameters [$\lambda_{pt}^f(I=1)$, λ_{pt}^m, and three amplitudes]. A detailed description of the fitting procedure will be published elsewhere [9]. We obtained

$$\lambda_{pt}^f(I=1) = 0.067 \pm 0.002^{+0.005}_{-0.002}\ \mu s^{-1},$$
$$\lambda_{pt}^m = 7.5 \pm 0.3^{+1.0}_{-0.3}\ \mu s^{-1}.$$

Here the second errors given denote the systematic errors, mainly due to the uncertainty of the pt-transfer rate [18–20]. The experimental value for λ_{pt}^m agrees with the calculated values $\lambda_{pt}^m = 6.5$ μs^{-1} [21] and $\lambda_{pt}^m = 6.38\,\mu$s^{-1} [22]. The rate for $pt\mu$ fusion is in agreement with the result from our earlier experiment [23]. The value $\lambda_{pt}^f(I=1) = 0.2\,\mu$s^{-1} derived in [24] from data on the pt reaction at low energies with the help of Eq. (4) and a value of $\rho_0 = 5.4 \times 10^{26}$ /cm^3 [25] is a factor of 3 larger than our experimental value. On the other hand our experimental value for $\lambda_{pt}^f(I=1)$ is an order of magnitude larger than the estimate [26] based on the reaction constant for the mirror reaction of radiative neutron capture by ^{3}He, $\lambda_{pt}^f(I=1) = 0.008\,\mu$s^{-1} [the cross section from the most recent experiment [27], $\sigma(n,\gamma) = 54 \pm 6\,\mu$b, is used]. This discrepancy is not yet understood.

From the mean of the conversion-muon disappearance rates (cf. line 12 of Table I), $\langle \lambda_d \rangle = 0.61 \pm 0.02\,\mu s^{-1}$, the rate for fusion from the $I = 0$ hyperfine state of the $pt\mu$ molecule was deduced to be $\lambda^f_{pt}(I = 0) = 0.15 \pm 0.02\,\mu s^{-1}$. This value is surprisingly large, namely more than 2 orders of magnitude larger than the most recent theoretical estimate [17], $\lambda^f_{pt}(I = 0) = 0.0005\,\mu s^{-1}$. Some work has to be done to clear this puzzle.

The data taken with the Ge(hp) detectors enabled us to deduce two quantities characterizing sticking after pt fusion: Our experimental value for the yield $\omega(K\alpha)$ of $K\alpha$ x rays from ^{4}He, $\omega(K\alpha) = (11 \pm 3)\%$ is in good agreement with the calculated value [28], $\omega(K\alpha) = 9.5\%$. Finally, the branching ratio B_{2p} of initial sticking in the $2p$ state over initial sticking in the $1s$ state of μ^4He was found to be $B_{2p} = (6.6 \pm 5.4)\%$.

We are indebted to H. Angerer, T. Ihn, M. L. Thomasek, H. Weiss, and the mechanical workshop of PSI for their valuable help. We wish to thank the accelerator crew of the GSF—Forschungszentrum für Umwelt und Gesundheit—in München-Neuherberg for giving us the opportunity to test our BGO detector. This work was supported by the German Federal Ministry of Research and Technology, the Austrian Academy of Sciences, and the Austrian Science Foundation.

[1] L. N. Bogdanova and V. E. Markushin, Muon Catal. Fusion **4**, 103 (1989).
[2] D. D. Bakalov, S. I. Vinitskii, and V. S. Melezhik, Zh. Eksp. Teor. Fiz. **79**, 1629 (1980) [Sov. Phys. JETP **52**, 820 (1980)].
[3] S. S. Gershtein, Zh. Eksp. Teor. Fiz. **40**, 698 (1961) [Sov. Phys. JETP **13**, 488 (1961)].
[4] E. J. Bleser *et al.*, Phys. Rev. **132**, 2679 (1963).
[5] A. V. Matveenko and L. I. Ponomarev, Zh. Eksp. Teor. Fiz. **58**, 1640 (1970) [Sov. Phys. JETP **31**, 880 (1970)].
[6] V. S. Melezhik, Muon Catal. Fusion **1**, 205 (1987).
[7] L. Bracci *et al.*, Phys. Lett. A **134**, 435 (1989).
[8] W. H. Breunlich *et al.*, Annu. Rev. Nucl. Part. Sci. **39**, 311 (1989).
[9] V. E. Markushin, P. Baumann, and F. J. Hartmann (to be published).
[10] P. U. Baumann, Ph.D. thesis, Technische Universität München, 1991.
[11] J. Zmeskal *et al.*, Muon Catal. Fusion **5/6**, 379 (1990/1991).
[12] H. Bossy *et al.*, Phys. Rev. Lett. **55**, 1870 (1985).
[13] E. I. Afanasieva, I. V. Balabin, and V. E. Markushin, Paul Scherrer Institute Report No. PR-90-17, 1990 (unpublished).
[14] E. I. Afanasieva, I. V. Balabin, and V. E. Markushin, Muon Catal. Fusion **5/6**, 477 (1990/1991).
[15] W. H. Breunlich *et al.*, Phys. Rev. Lett. **58**, 329 (1987).
[16] W. H. Breunlich *et al.*, Muon Catal. Fusion **1**, 121 (1987).
[17] L. Bogdanova and V. E. Markushin, Nucl. Phys. **A508**, 29c (1990).
[18] M. Bubak and M. P. Faifman, Report No. JINR E4-87-464, 1987 (to be published).
[19] J. S. Cohen and M. C. Struensee, Phys. Rev. A **43**, 3460 (1991).
[20] C. Chiccoli *et al.*, Muon Catal. Fusion **7**, 87 (1992).
[21] L. I. Ponomarev and M. P. Faifman, Zh. Eksp. Teor. Fiz. **71**, 1689 (1976) [Sov. Phys. JETP **44**, 886 (1976)].
[22] M. P. Faifman, Muon Catal. Fusion **4**, 341 (1989).
[23] F. J. Hartmann *et al.*, Muon Catal. Fusion **2**, 53 (1988).
[24] L. Bogdanova, International Workshop on Muon Catalyzed Fusion, μCF-92, Uppsala, 1992 (unpublished).
[25] S. A. Alexander, P. Froelich, and H. Monkhorst, Phys. Rev. A **41**, 2854 (1990).
[26] J. D. Jackson (private communication).
[27] F. L. H. Wolfs *et al.*, Phys. Rev. Lett. **63**, 2721 (1989).
[28] V. E. Markushin, Muon Catal. Fusion **3**, 395 (1988).